Supporting Information

A Recyclable Carbon Nanoparticles-Based Fluorescent Probe for Highly Selective and Sensitive Detection of Mercapto Biomolecules

Minhuan Lan, Jinfeng Zhang, Ying-San Chui, Hui Wang, Qingdan Yang, Xiaoyue Zhu, Huaixin Wei, Weimin Liu, Jiechao Ge, Pengfei Wang, Xianfeng Chen, Chun-Sing Lee, and Wenjun Zhang**

Table S1. CNPs based fluorescence sensor toward thiols compounds.

Methods	Respone time	pH range	PL Quenching efficiency	PL recovering efficiency	Circu-larity test	Ref.
C-dots-Hg^{2+}	5 min	7.5~9.5	~60%	~30%	N/A	[R1]
C-dots-Au NPs	5 min	N/A	N/A	~25%	N/A	[R2]
C-dots-Cu^{2+}	1 min	5.0~6.0	~90%	~80%	N/A	[R3]
GQDs-Hg^{2+}	N/A	7.0~7.4	~93%	~95%	N/A	[R4]
GQDs-Ag NPs	5 min	6.5~9.5	~40%	N/A	N/A	[R5]
CNPs-Hg^{2+}	**10 s**	**5.0~10.0**	**98.7%**	**93.2%**	**10**	**This work**

[R1] L. Zhou, Y. H. Lin, Z. Z. Huang, J. S. Ren and X. G. Qu, *Chem. Commun.*, 2012, **48**, 1147.
[R2] Y. P. Shi, Y. Pan, H. Zhang, Z. M. Zhang, M. J. Li, C. Q. Yi and M. S. Yang, *Biosens. Bioelectron.*, 2014, **56**, 39.
[R3] H. Z. Zheng, W. J. Bai, Y. J. Long, M. Gao and L. Y. Zhang, *Scientia Sinica Chimica.,* 2011, **41**, 1031.
[R4] Z. Z. Wu, W. Y. Li, J. Chen and C. Yu, *Talanta,* 2014, **119**, 538.
[R5] X. Ran, H. J. Sun, F. Pu, J. S. Ren and X. G. Qu, *Chem. Commun.*, 2013, **49**, 1079.

Table S2. The influence of synthesis parameters on the properties of CNPs.

	Reaction temperature (°C)	Reaction time (h)	Citrate trisodium /Melamine	Quenching efficiency (%)	Recovering efficiency (%)	QY @330 nm	QY @340 nm	QY @350 nm
CNPs-A	160	12	2	97.7	77.8	0.31	0.31	0.33
CNPs-B	180	3	2	95.4	73.1	0.31	0.32	0.34
CNPs-C	180	6	2	97.6	74.5	0.35	0.35	0.36
CNPs-D	180	12	2	98.7	93.2	0.30	0.31	0.34
CNPs-E	180	24	2	95.0	91.1	0.27	0.29	0.31
CNPs-F	180	12	1	97.6	75.6	0.33	0.35	0.36
CNPs-G	180	12	0.5	94.4	81.8	0.28	0.30	0.32

Data notes:

1. Quenching efficiency and recovering efficiency were calculated from the following equations:

Quenching efficiency (%) = $(I_0-I_{Hg})*100/I_0$;

Recovering efficiency (%) = $I_{Cys}*100/I_0$

where I_0 is the PL intensity of CNPs at 437 nm in the absence of Hg^{2+} and Cys. I_{Hg} and I_{Cys} refer to the PL intensity of CNPs at 437 nm in the presence of 10 μM Hg^{2+} and 20 μM Cys, respectively.

2. The QY was determined by the reference of quinine sulfate (QY = 0.54 when in 0.1 M H_2SO_4 aqueous solution) at different excitation wavelengths (330, 340 and 350 nm).

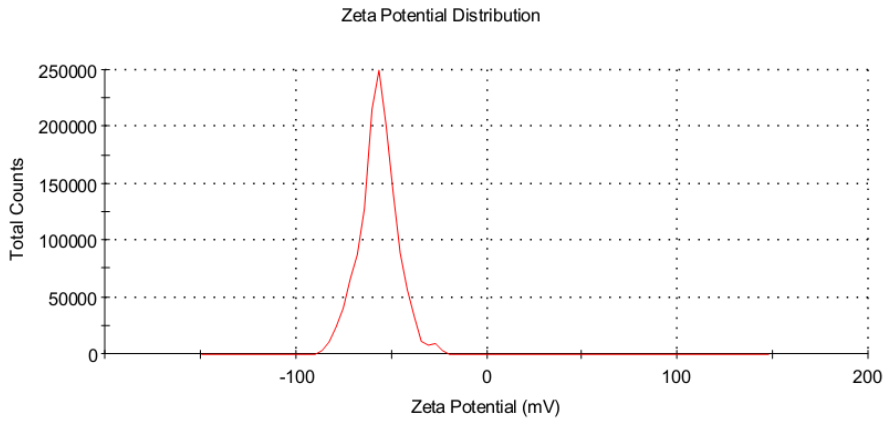

Fig. S1. Zeta-potential spectrum of CNPs.

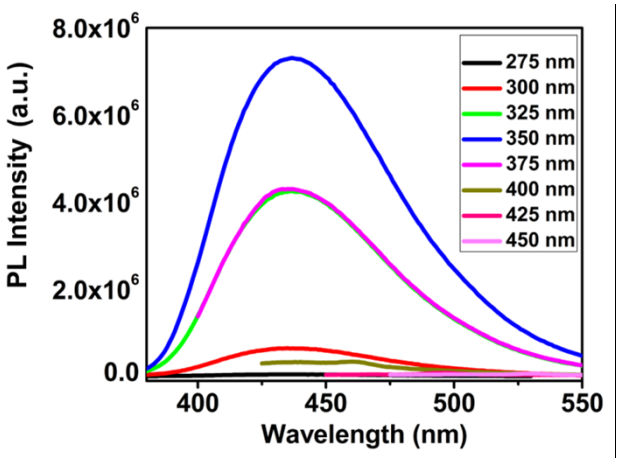

Fig. S2. PL spectra of CNPs aqueous solution under excitation with different wavelengths from 275 to 450 nm.

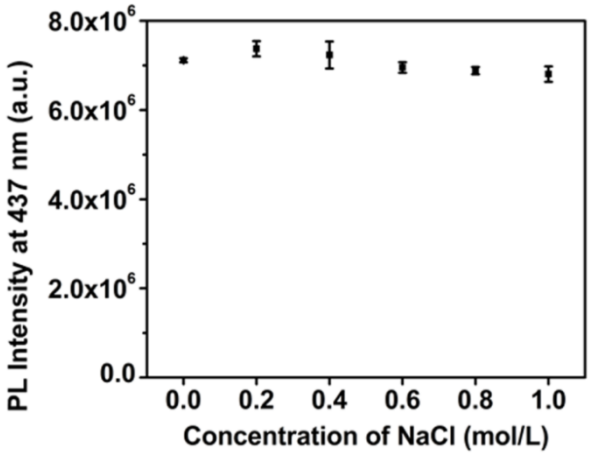

Fig. S3. The PL intensities of CNPs aqeuous solution at 437 nm at different NaCl concentrations (0, 0.2, 0.4, 0.6, 0.8, 1.0 mol/L).

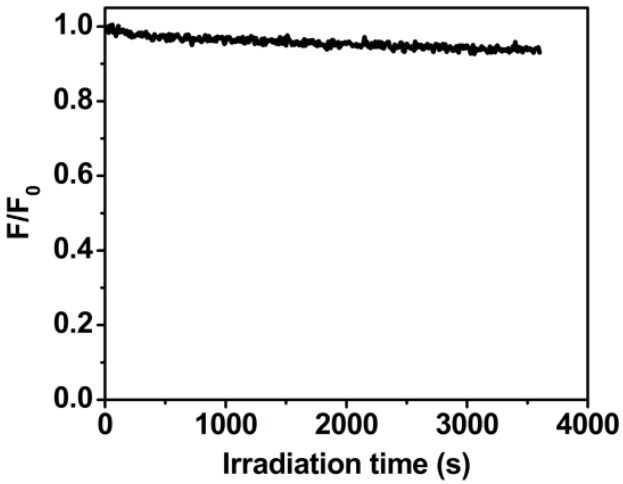

Fig. S4. Photostability of CNPs aqueous solution evaluated by the 350 nm xenon lamp equipped in the FL spectrometer. F_0 and F represent the fluorescent intensity of CNPs at 437 nm before and after irradiation, respectively.

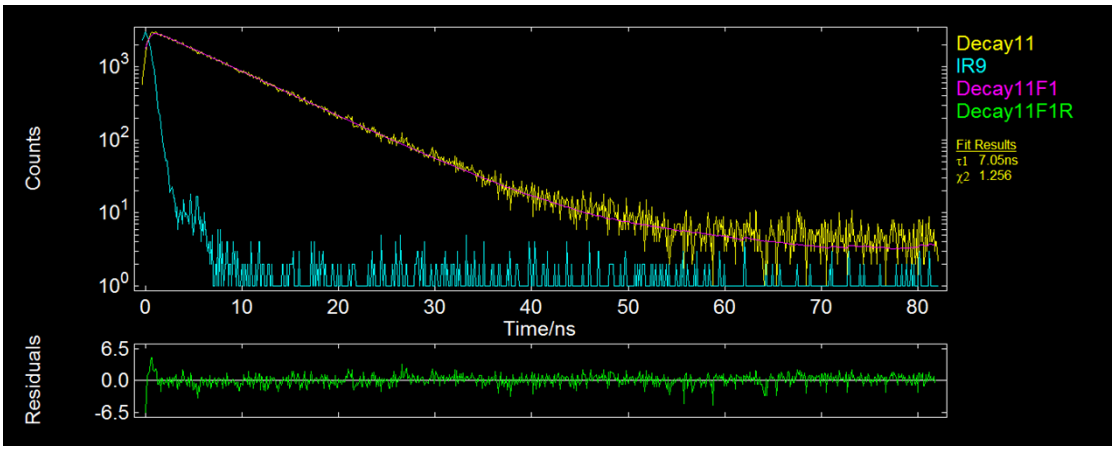

Fig. S5. Fluorescence decay curve (yellow line) of CNPs recorded at 437 nm with the excitation of 355 nm. Blue line: the instrument noise; and red line: fitting of the fluorescence decay curve. Fit = $A+B_1\exp(-t/\tau_1)$, (τ_1=7.0 ns).

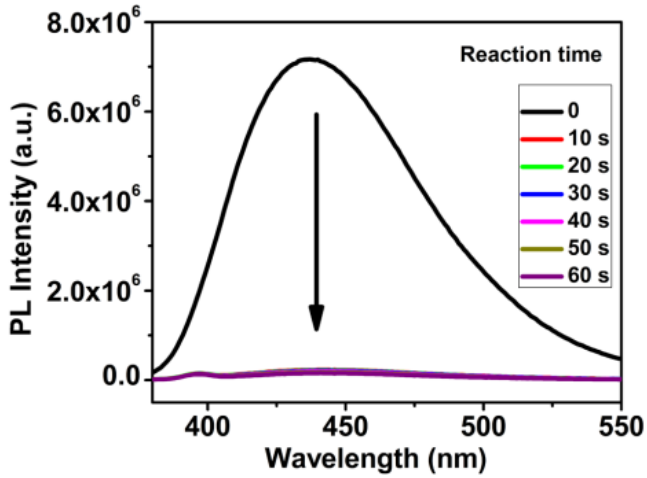

Fig. S6. Time-dependent PL spectra of CNPs upon addition of 10 μM Hg^{2+} in HEPES buffer solution at room temperature (λ_{ex}=350 nm).

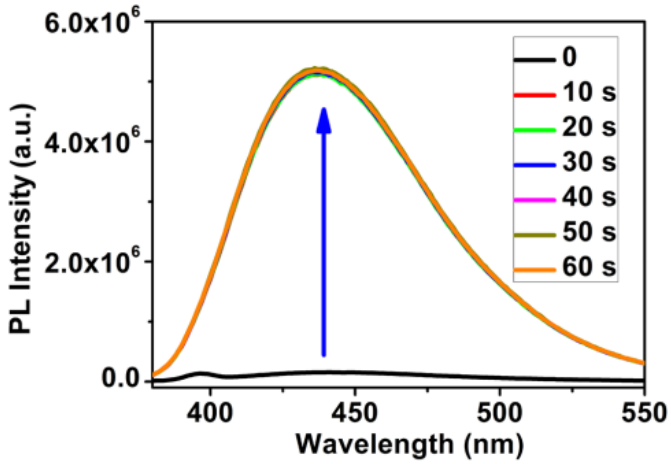

Fig. S7. Time-dependent PL spectra of CNPs-Hg^{2+} system upon addition of 10 μM Cys in HEPES buffer solution at room temperature (λ_{ex}=350 nm).

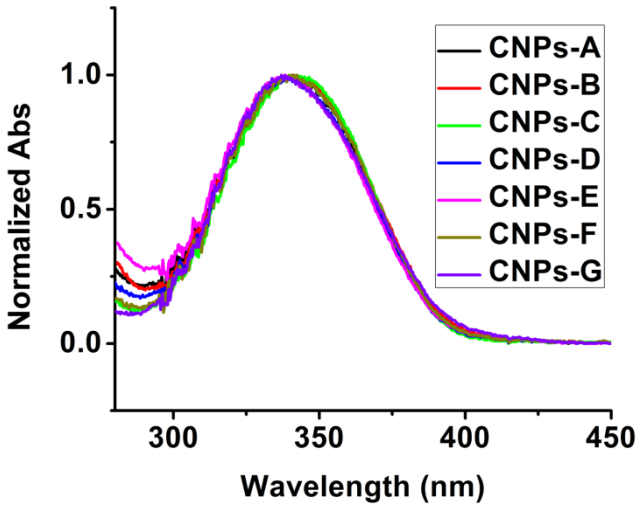

Fig. S8. Normalized UV-vis spectra of CNPs prepared under different conditions.

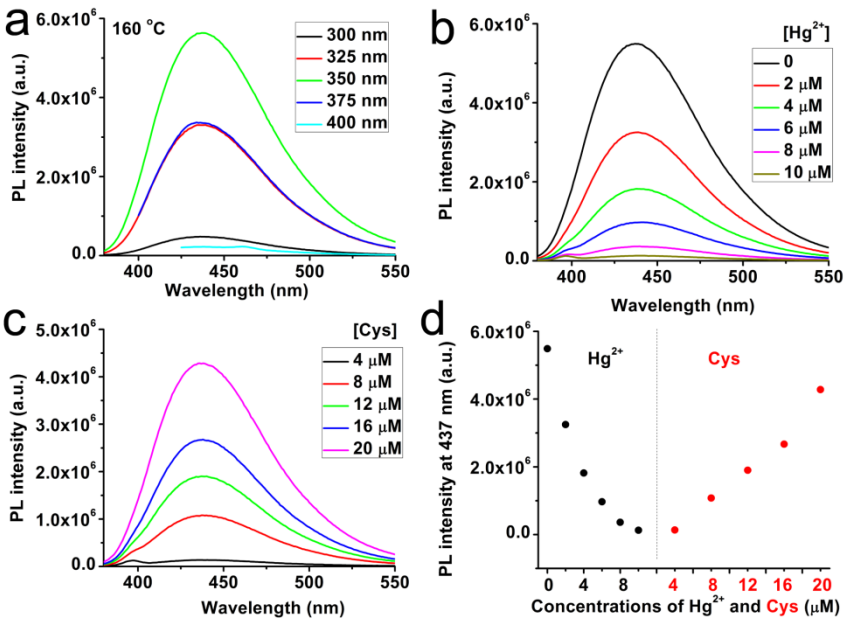

Fig. S9A. (a) PL spectra of CNPs-A aqueous solution under excitation with different wavelengths from 300 to 400 nm. (b) Dependence of PL spectra of CNPs-A in HEPES buffer solution (10 mM, pH 7.2) on the gradual addition of Hg^{2+} from 0 to 10 μM and (c) following addition of Cys from 4 to 20 μM. (λ_{ex}=350 nm). (d) Dependence of PL intensity at 437 nm with incremental addition of Hg^{2+} and Cys.

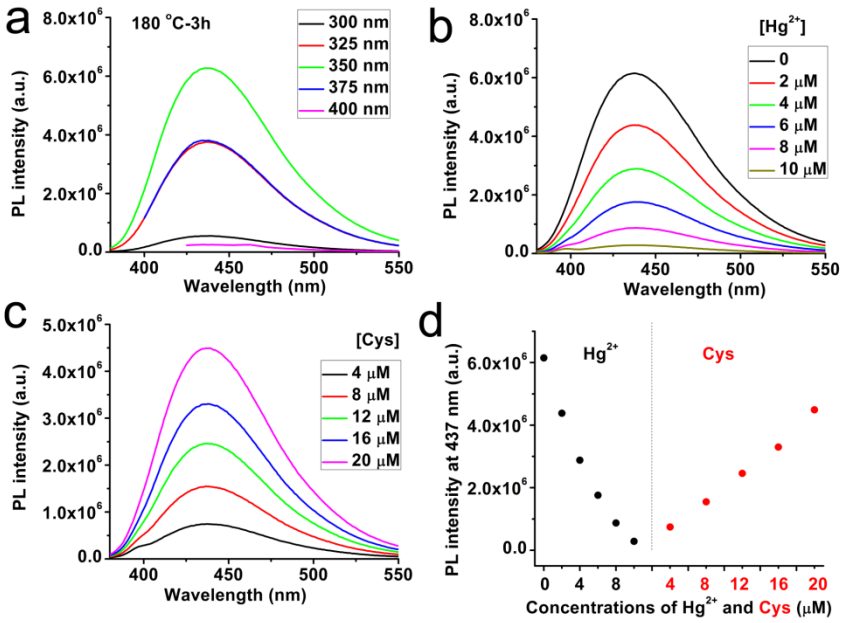

Fig. S9B. (a) PL spectra of CNPs-B aqueous solution under excitation with different wavelengths from 300 to 400 nm. (b) Dependence of PL spectra of CNPs-B in HEPES buffer solution (10 mM, pH 7.2) on the gradual addition of Hg^{2+} from 0 to 10 μM and (c) following addition of Cys from 4 to 20 μM. (λ_{ex}=350 nm). (d) Dependence of PL intensity at 437 nm with incremental addition of Hg^{2+} and Cys.

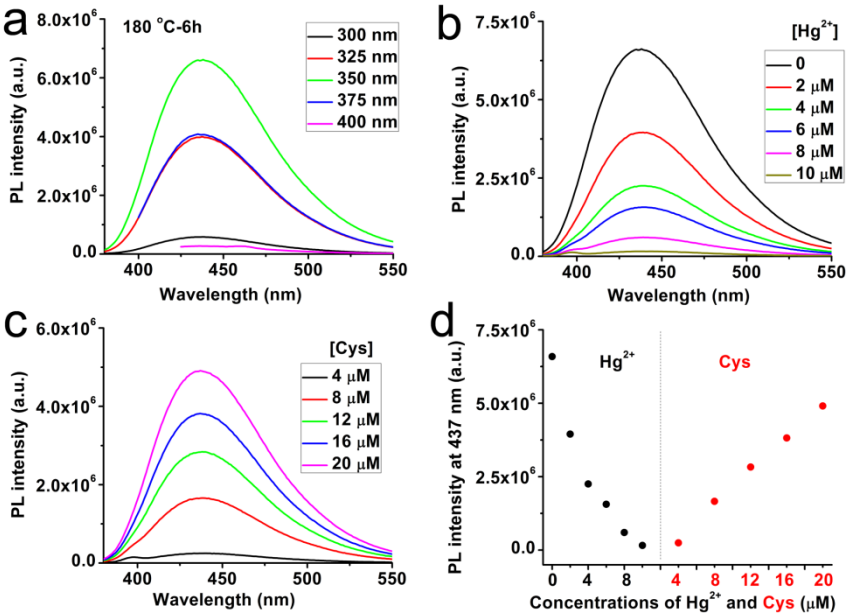

Fig. S9C. (a) PL spectra of CNPs-C aqueous solution under excitation with different wavelengths from 300 to 400 nm. (b) Dependence of PL spectra of CNPs-C in HEPES buffer solution (10 mM, pH 7.2) on the gradual addition of Hg^{2+} from 0 to 10 μM and (c) following addition of Cys from 4 to 20 μM. (λ_{ex}=350 nm). (d) Dependence of PL intensity at 437 nm with incremental addition of Hg^{2+} and Cys.

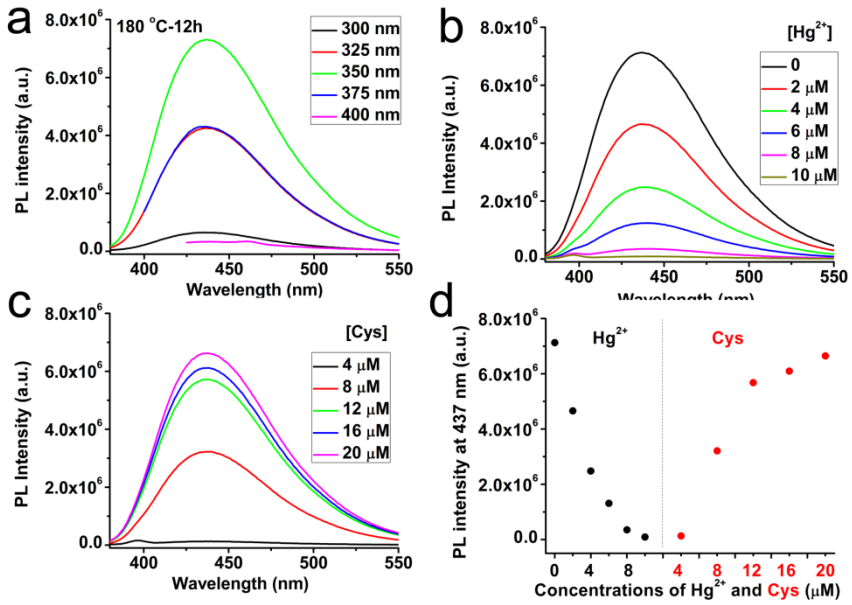

Fig. S9D. (a) PL spectra of CNPs-D aqueous solution under excitation with different wavelengths from 300 to 400 nm. (b) Dependence of PL spectra of CNPs-D in HEPES buffer solution (10 mM, pH 7.2) on the gradual addition of Hg^{2+} from 0 to 10 μM and (c) following addition of Cys from 4 to 20 μM. (λ_{ex}=350 nm). (d) Dependence of PL intensity at 437 nm with incremental addition of Hg^{2+} and Cys.

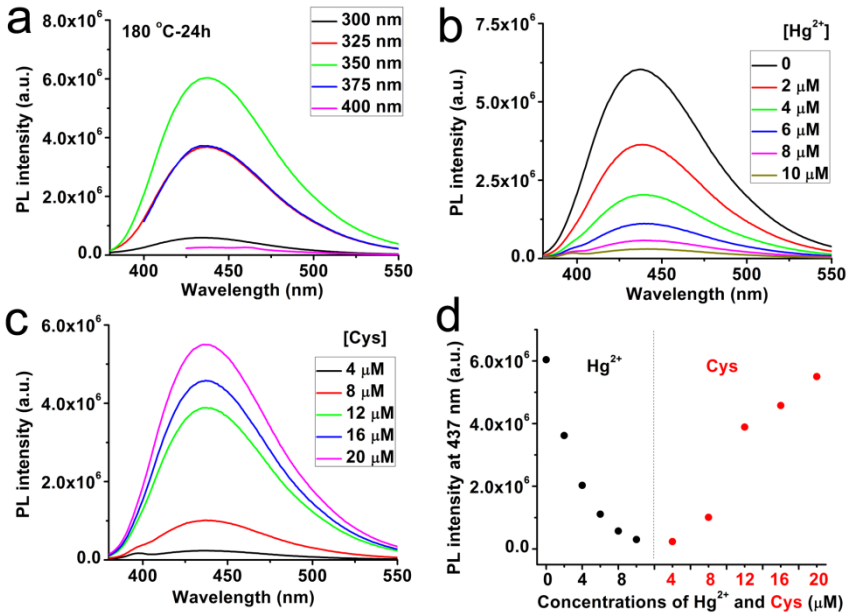

Fig. S9E. (a) PL spectra of CNPs-E aqueous solution under excitation with different wavelengths from 300 to 400 nm. (b) Dependence of PL spectra of CNPs-E in HEPES buffer solution (10 mM, pH 7.2) on the gradual addition of Hg^{2+} from 0 to 10 μM and (c) following addition of Cys from 4 to 20 μM. (λ_{ex}=350 nm). (d) Dependence of PL intensity at 437 nm with incremental addition of Hg^{2+} and Cys.

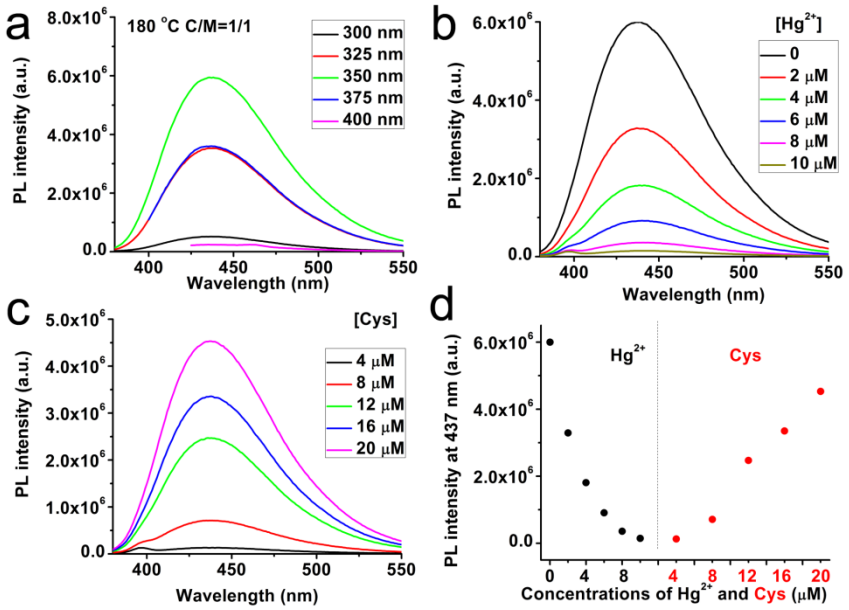

Fig. S9F. (a) PL spectra of CNPs-F aqueous solution under excitation with different wavelengths from 300 to 400 nm. (b) Dependence of PL spectra of CNPs-F in HEPES buffer solution (10 mM, pH 7.2) on the gradual addition of Hg^{2+} from 0 to 10 μM and (c) following addition of Cys from 4 to 20 μM. (λ_{ex}=350 nm). (d) Dependence of PL intensity at 437 nm with incremental addition of Hg^{2+} and Cys.

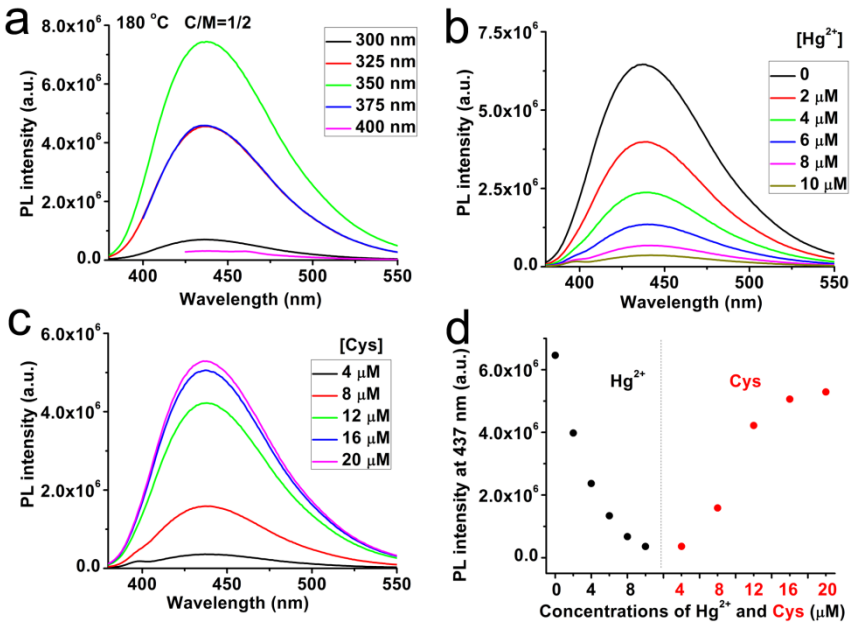

Fig. S9G. (a) PL spectra of CNPs-G aqueous solution under excitation with different wavelengths from 300 to 400 nm. (b) Dependence of PL spectra of CNPs-G in HEPES buffer solution (10 mM, pH 7.2) on the gradual addition of Hg^{2+} from 0 to 10 μM and (c) following addition of Cys from 4 to 20 μM. (λ_{ex}=350 nm). (d) Dependence of PL intensity at 437 nm with incremental addition of Hg^{2+} and Cys.

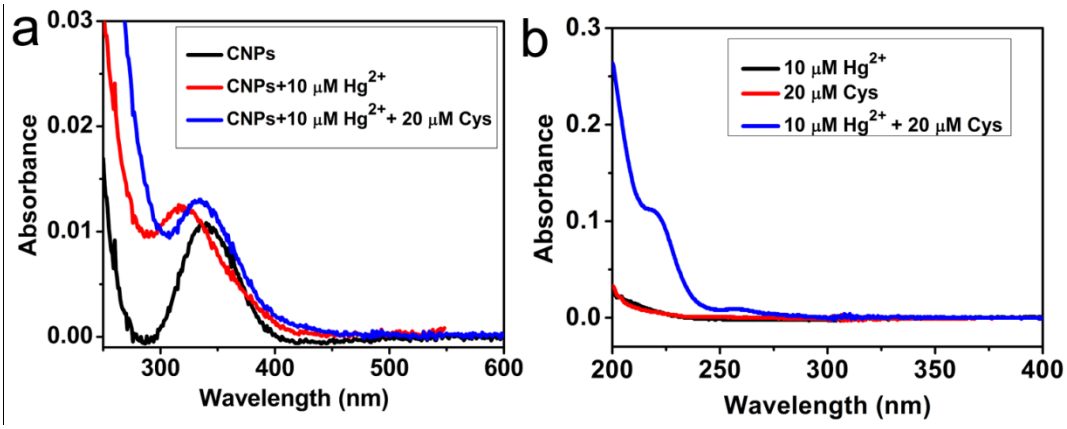

Fig. S10. (a) Absorption spectra of CNPs (black line), CNPs-Hg^{2+} (red line) and CNPs-Hg^{2+}-Cys mixture (blue line) in HEPES buffer solutions (10 mM, pH 7.2). (b) Absorption spectra of 10 μM $HgCl_2$ (black line), 20 μM Cys (red line) and the mixture of $HgCl_2$ and Cys (blue line) in HEPES buffer solutions (10 mM, pH 7.2).

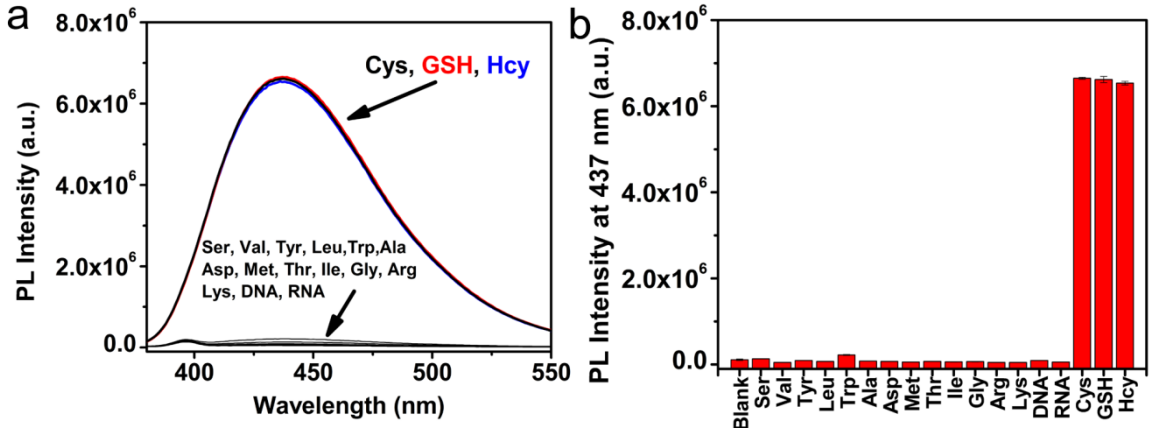

Fig. S11. (a) PL spectra and (b) the corresponding PL intensities at 437 nm of CNPs-Hg^{2+} solutions with the addition of amino acids, DNA and RNA in HEPES buffer solution (λ_{ex}=350 nm). The concentration of these analytes was 20 μM.

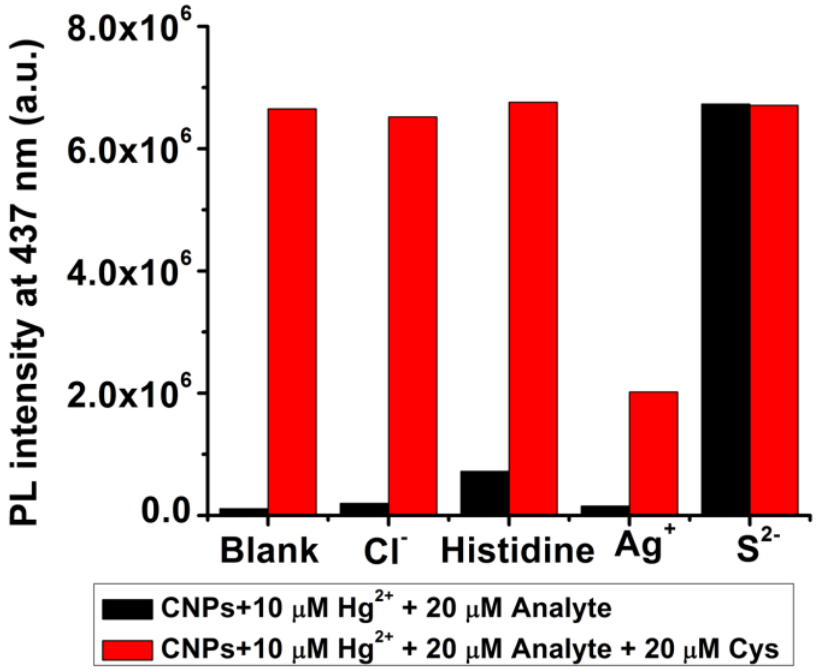

Fig. S12. Selectivity of CNPs-Hg^{2+} system to Cys in the presence of 20 μM Cl^-, histidine, Ag^+ and S^{2-} in HEPES buffer solution (10 mM, pH 7.2). Blank refer to the free CNPs-Hg^{2+} aqueous solution.

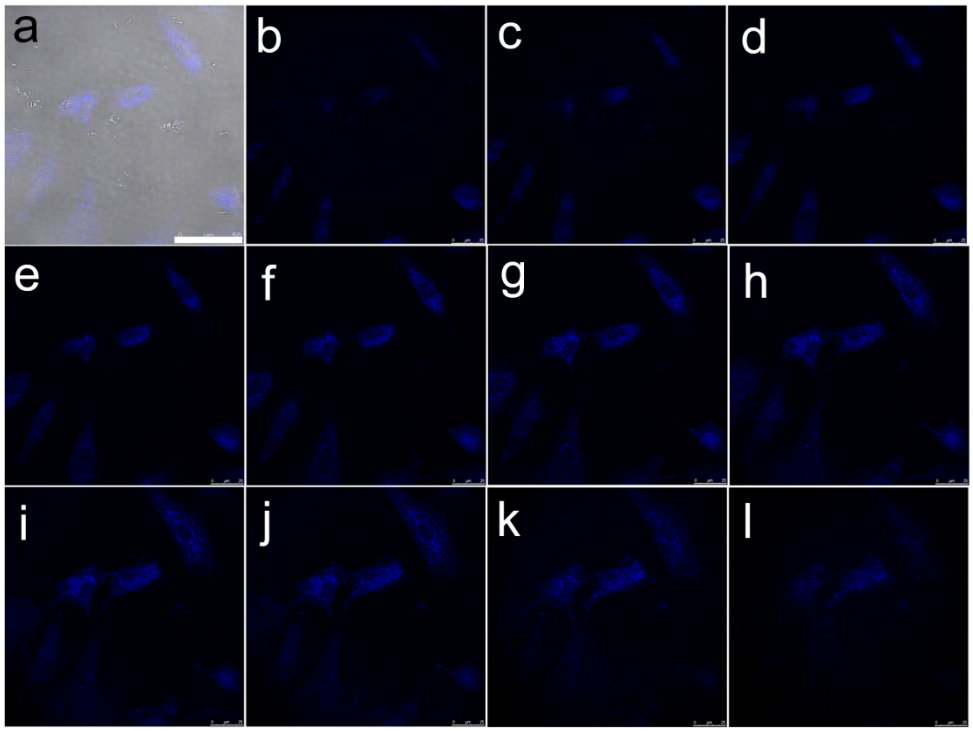

Fig. S13. Confocal laser scanning microscopy z-stack images of A549 cell incubated with CNPs (λ_{ex}=405 nm). (a) The overlay of bright field and fluorescence images. (b)~(l) Z-stack scanning mode images from the top to the bottom of cells. The scale bar is 50 μm.

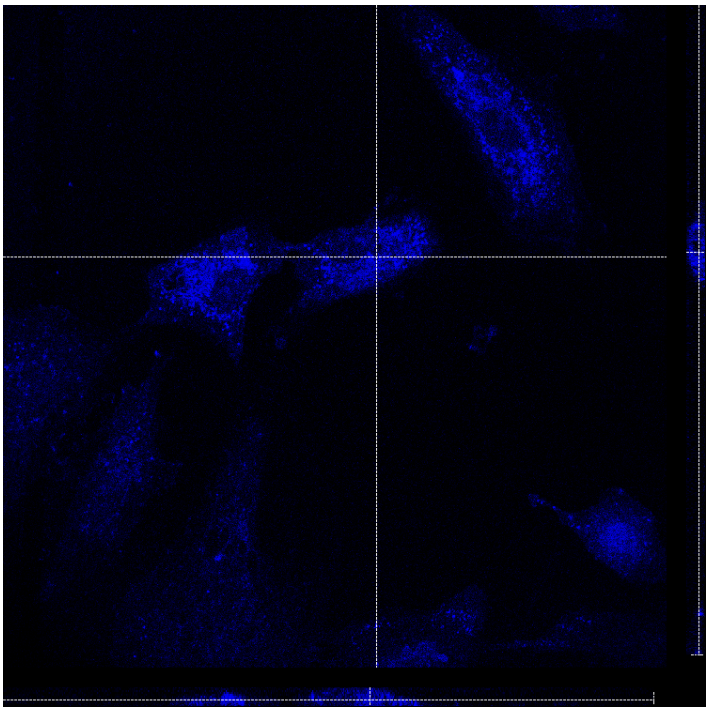

Fig. S14. Confocal microscopy images of multiple cross-sections exhibiting various locations of CNPs within A549 cells.